

# Dalton Transactions

Accepted Manuscript



This is an *Accepted Manuscript*, which has been through the Royal Society of Chemistry peer review process and has been accepted for publication.

*Accepted Manuscripts* are published online shortly after acceptance, before technical editing, formatting and proof reading. Using this free service, authors can make their results available to the community, in citable form, before we publish the edited article. We will replace this *Accepted Manuscript* with the edited and formatted *Advance Article* as soon as it is available.

You can find more information about *Accepted Manuscripts* in the [Information for Authors](#).

Please note that technical editing may introduce minor changes to the text and/or graphics, which may alter content. The journal's standard [Terms & Conditions](#) and the [Ethical guidelines](#) still apply. In no event shall the Royal Society of Chemistry be held responsible for any errors or omissions in this *Accepted Manuscript* or any consequences arising from the use of any information it contains.



Journal Name

ARTICLE

## Oxidative photoreactivity of mono-transition-metal functionalized lacunary Keggin anions

M. Dave<sup>a</sup>, and C. Streb<sup>a\*</sup>

Received 00th January 20xx,

Accepted 00th January 20xx

DOI: 10.1039/x0xx00000x

www.rsc.org/

A comparative study investigating the effects of metal substitution on the photocatalytic activity of metal oxide cluster anions is presented. The study shows that metal functionalization can be used to alter the photochemical properties of monolacunary tungstate - based Keggin clusters ( $\alpha$ -[TM(H<sub>2</sub>O)SiW<sub>11</sub>O<sub>39</sub>]<sup>n-</sup> (M = Co<sup>2+</sup>, Cu<sup>2+</sup>, Ni<sup>2+</sup>, Mn<sup>2+</sup>). It is demonstrated that the photoactivity for the photooxidation of the model pollutant basic blue 41 is dependent of the type of metal employed and increases in the order Co < Cu < Ni < Mn under aerobic conditions and 390 nm monochromatic irradiation. A significant increase of the reaction rate is observed under aerated conditions compared with de-aerated conditions, suggesting that oxygen serves as a re-oxidant for the reduced clusters. Radical scavenging experiments suggest that the photocatalysis proceeds via formation of hydroxyl radicals.

### Introduction

Polyoxometalates (POMs) are discrete anionic metal–oxygen clusters (generally based on early transition metals in their highest oxidation states) formed in solution by self-assembly of oxometalate precursors [MO<sub>x</sub>]<sup>n-</sup>.<sup>1–3</sup> POMs feature an unmatched range of tuneable physical and chemical properties, making them the focus of new applications in catalysis,<sup>4</sup> photocatalysis,<sup>5</sup> molecular magnetism and electronics,<sup>6</sup> material science<sup>7</sup> and sustainable energy research.<sup>8</sup>

To-date, a wide range of synthetic procedures allows the incorporation of almost any chemical element into the metal-oxo framework of POMs, giving unique options to tune chemical reactivity on the atomic level. One highly active area of research is the tuning of the photocatalytic properties of POMs.<sup>5</sup> Typically, the photochemistry of POMs is dominated by strong ligand to metal charge transfer (LMCT) transitions located in the UV and (more rarely) in the near visible spectral range.<sup>9</sup> Several strategies such as structural cluster modifications,<sup>10</sup> the incorporation of photosensitizers<sup>11</sup> and incorporation of heterometals<sup>12</sup> have been

proposed to modify the photochemical reactivity of POMs, often with a view of changing the photooxidative activity/selectivity<sup>13</sup> and the visible light activity<sup>14</sup> of the clusters.

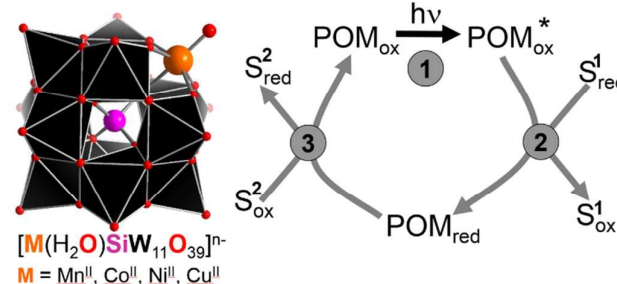


**Figure 1** Left: Illustration of the transition metal functionalized Keggin anion employed as (photo-)catalyst. right: typical POM-catalyzed photoredox-cycle. S<sup>1</sup>, S<sup>2</sup>: substrates.<sup>5</sup>

Recently, we showed that incorporation of vanadium(V) centers into molybdate(VI) and tungstate(VI)-based Lindqvist anions [V<sub>x</sub>M<sub>6-x</sub>O<sub>19</sub>]<sup>(2+x)-</sup> (x = 0,1,2; M = Mo(VI), W(VI)) results in improved photoreactivity in the UV and VIS range.<sup>14,15</sup> The introduction of V<sup>V</sup> centres leads to lower-lying metal-centered LUMO levels, resulting in a decreased HOMO-LUMO gap and thus increased VIS light absorption.

A different class of POMs where metal substitution has been developed to great effect are lacunary Keggin anions such as the mono-lacunary species [SiW<sub>11</sub>O<sub>39</sub>]<sup>8-</sup> (= {W<sub>11</sub>}).<sup>16</sup> Incorporation of various metals M into the vacant binding site of {W<sub>11</sub>} results in the

<sup>a</sup> Institute of Inorganic Chemistry I, Ulm University, Albert-Einstein-Allee 11, 89081 Ulm, Germany, carsten.streb@uni-ulm.de; www.strebgroup.net

Electronic Supplementary Information (ESI) available: [details of any supplementary information available should be included here]. See DOI: 10.1039/x0xx00000x

formation of metal-functionalized species  $[M(H_2O)W_{11}O_{39}]^{n-}$  ( $\{MW_{11}\}$ ), see Fig. 1.<sup>17–19</sup> This approach has been successfully used to access new materials for catalysis,<sup>20</sup> materials design<sup>21</sup> and molecular magnetism.<sup>22</sup>

**Table 1** Summary of photocatalysts used

No	Formula	Abbreviation	$\epsilon_{390\text{ nm}} / \text{M}^{-1}\text{cm}^{-1}$ <sup>a</sup>
1	$(n\text{Bu}_4\text{N})_6[\alpha\text{-SiW}_{11}\text{O}_{39}\text{Cu}(\text{H}_2\text{O})]$	$\{\text{CuW}_{11}\}$	32.1
2	$(n\text{Bu}_4\text{N})_6[\alpha\text{-SiW}_{11}\text{O}_{39}\text{Co}(\text{H}_2\text{O})]$	$\{\text{CoW}_{11}\}$	144.2
3	$(n\text{Bu}_4\text{N})_6[\alpha\text{-SiW}_{11}\text{O}_{39}\text{Ni}(\text{H}_2\text{O})]$	$\{\text{NiW}_{11}\}$	78.7
4	$(n\text{Bu}_4\text{N})_6[\alpha\text{-SiW}_{11}\text{O}_{39}\text{Mn}(\text{H}_2\text{O})]$	$\{\text{MnW}_{11}\}$	78.5

<sup>a</sup> molar extinction coefficients determined in N,N-dimethyl formamide (DMF) solution

Here, we investigate the effects of  $\{W_{11}\}$ -metal functionalization on the photooxidative activity of the cluster under homogeneous conditions. To this end, a series of metal-functionalized species  $\{MW_{11}\}$  ( $M = \text{Mn}^{\text{II}}, \text{Co}^{\text{II}}, \text{Ni}^{\text{II}}, \text{Cu}^{\text{II}}$ , see Table 1) were synthesized and isolated as organo-soluble  $n\text{Bu}_4\text{N}^+$  salts according to reported procedures.<sup>19</sup> The photochemical properties and photooxidative performance of the compounds were evaluated using a standardized dye decomposition<sup>14,15,23,24</sup> (model dye: basic blue 41, BB41) as benchmark reaction. The photochemical reactivity was investigated at the UV-Vis border ( $\lambda_{\text{irradiation}} = 390\text{ nm}$ ) to establish the catalyst performance with high energy near UV/visible light. Several aspects of the photooxidation mechanism such as the presence of oxygen and hydroxyl radical scavengers were studied to evaluate the cluster reactivity.

## Results and discussion

**Synthesis and characterization:** The compounds  $\{MW_{11}\}$  were obtained by modified literature syntheses (see ESI for details).<sup>19</sup> The compounds were isolated as organo-soluble salts using tetra-*n*-butylammonium counter ions. The compounds were characterized using UV-Vis- and FT-IR-spectroscopy and elemental analysis, see ESI.

**UV-Vis spectroscopy:** UV-Vis spectroscopy of  $\{MW_{11}\}$  showed that all clusters feature O–M ligand to metal charge-transfer (LMCT) transitions in the UV region and tailing of the near UV-Vis transitions up to ca. 400 nm was observed, see Figure 2. All  $\{MW_{11}\}$  clusters also show distinct band features in the UV range between 250–350 nm, suggesting that the electronic cluster structure is modified by transition metal incorporation.<sup>14</sup>

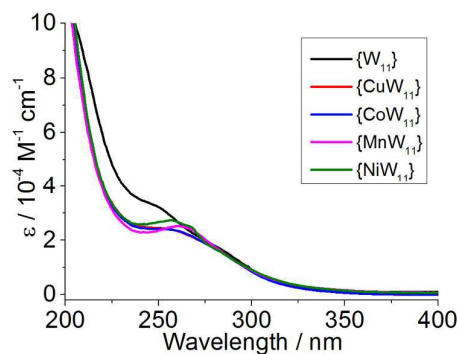


**Figure 2** UV – Vis spectra of  $\{W_{11}\}$  (in MeCN) and  $\{MW_{11}\}$  (in DMF), showing the effect of transition metal substitution on the UV-visible light absorption.

**Catalytic activity under non-irradiated conditions:** The “background” oxidative activity of the  $\{MW_{11}\}$  clusters was initially determined under dark, non-irradiated reaction conditions in aerated N,N-dimethyl formamide (DMF) solutions. To this end, a standardized catalytic protocol was used: the catalysts (4.0  $\mu\text{M}$ ) were dissolved in aerated DMF and aliquots of the model dye BB41 were added at molar ratios  $[\text{BB41}]:[\text{cluster}] = 5:1$ . Dye degradation was followed as a function of time using UV-Vis spectrophotometry. For all metal-functionalized  $\{MW_{11}\}$  species employed, light-independent oxidative catalytic activity was observed and observed pseudo first-order reaction rates  $k_{\text{obs}}$  were determined. Briefly, the catalytic activity under non-irradiated conditions is dependent of the metal employed and increases in the order  $\text{Ni} < \text{Cu} < \text{Co} < \text{Mn}$ , see Table 2. The non-substituted  $\{W_{11}\}$  showed no oxidative reactivity and only minimal dye degradation was observed in the absence of any catalyst.

**Table 2** Observed pseudo-first order rate constants for  $\{W_{11}\}$  and  $\{MW_{11}\}$  for the aerated BB41 photooxidation under non-irradiated and irradiated (390 nm) conditions.

No	Cluster	Aerated, non-irradiated $k_{\text{obs}} / 10^{-8} \text{ M min}^{-1}$	Aerated, irradiated $k_{\text{obs}} / 10^{-8} \text{ M min}^{-1}$	% increase under irradiation
	–	$0.07 \pm 0.05$	$0.19 \pm 0.04$	–
1	$\{W_{11}\}$	n.d.	$0.51 \pm 0.08$	–
2	$\{\text{CuW}_{11}\}$	$0.38 \pm 0.02$	$4.66 \pm 0.13$	1126
3	$\{\text{CoW}_{11}\}$	$0.88 \pm 0.07$	$5.17 \pm 0.17$	488
4	$\{\text{NiW}_{11}\}$	$0.25 \pm 0.01$	$5.33 \pm 0.28$	2032
5	$\{\text{MnW}_{11}\}$	$1.45 \pm 0.14$	$9.59 \pm 0.34$	561

**Photocatalytic studies:** In the next series of experiments, the photocatalytic activity of the  $\{MW_{11}\}$  clusters was investigated. To this end, the standard dye decomposition reaction described above was carried out with additional irradiation with monochromatic light (LED light source,  $\lambda_{\text{max}} = 390\text{ nm}$ ).

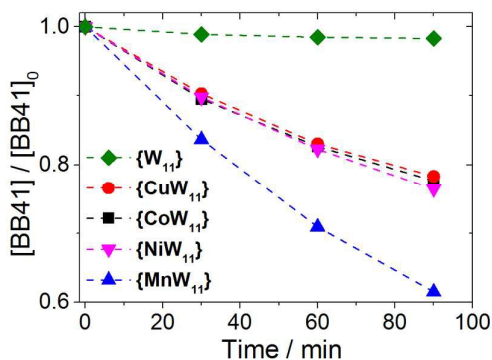


**Figure 3** Photochemical BB41 oxidation by  $\{MW_{11}\}$  and  $\{W_{11}\}$  in DMF under aerated conditions. Conditions: [catalyst] = 4.0  $\mu$ M, [BB41]<sub>0</sub> = 20  $\mu$ M, 390 nm LED irradiation.

Under aerated conditions (the solvent was allowed to equilibrate in air before the measurements), an increased oxidative reactivity was observed for all  $\{MW_{11}\}$  clusters compared with the reactivity under non-irradiated conditions. Cluster reactivity for the BB41 photooxidation increased in the order Cu < Co < Ni < Mn (Figure 3). Notably, the rate constants for Cu, Co and Ni all fall within the same range whereas the rate constant for Mn is almost twice as high, see Table 2.

When comparing the reactivity of the non-irradiated references with the irradiated samples, increased reactivity is observed for all  $\{MW_{11}\}$  species. Rate constant increases between ca. 500 and 2000 % are observed.  $\{NiW_{11}\}$ , which is the least reactive metal-substituted species under non-irradiated conditions, shows the most significant increase in reactivity, making it comparable to the Cu and Co species under irradiated conditions (Table 2).

$\{MnW_{11}\}$  shows the highest oxidative activity under the given experimental setting, both for non-irradiated and irradiated conditions. Note that the observed difference in photocatalytic activity of the  $\{MW_{11}\}$  clusters is not related to their light absorption at the irradiation wavelength (see Table 1), as all species feature similar molar extinction coefficients. Instead, the difference in reactivity is most likely associated with the redox-active metal centre present. Future studies will investigate the reactivity difference using transient absorption spectroscopy and related photophysical measurements.

**Mechanistic studies:** Initial mechanistic analyses were performed to shed light on the underlying reaction mechanisms. To this end, the standard dye degradation was investigated under de-aerated conditions (the samples were flushed with argon before irradiation). De-aerated experiments were performed for the dark and irradiated reaction. In all cases, a decrease in reaction rate compared with the aerated samples was observed, see Figure 4 and Table 3.

The rate reduction under irradiated, de-aerated conditions was in the range between ca. 57 % for  $\{NiW_{11}\}$  and ca. 92 % for  $\{CoW_{11}\}$ . The data suggest that oxygen is required for efficient photocatalytic activity and is most likely required for the re-oxidation of the reduced cluster species, see Fig. 1. This

is in line with previous reports where similar behaviour was found.<sup>15,23,25</sup>

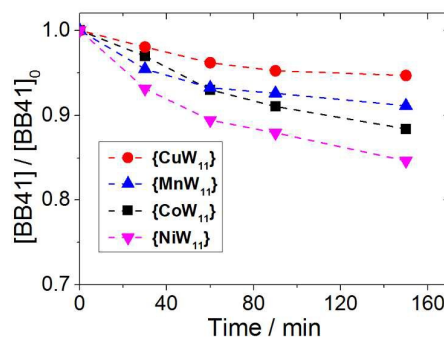


**Figure 4** Photochemical BB41 oxidation by  $\{MW_{11}\}$  in DMF under de-aerated conditions. Conditions:  $\{MW_{11}\}$  = 4.0  $\mu$ M, [BB41]<sub>0</sub> = 20  $\mu$ M, 390 nm LED irradiation. Samples were degassed with Ar for 10 min prior to the experiment.

**Table 3** Observed rate constants for the  $\{MW_{11}\}$  photocatalyzed oxidation of BB41 under de-aerated conditions.<sup>a</sup>

No	Cluster	Deaerated, non-irradiated $k_{obs}$ / $10^{-8}$ M min <sup>-1</sup>	De-aerated, irradiated $k_{obs}$ / $10^{-8}$ M min <sup>-1</sup>	Percent decrease <sup>b</sup>
1	$\{CuW_{11}\}$	0.35 ± 0.02	1.69 ± 0.14	63.73
2	$\{CoW_{11}\}$	0.11 ± 0.03	0.43 ± 0.01	91.68
3	$\{NiW_{11}\}$	0.10 ± 0.05	2.27 ± 0.19	57.41
4	$\{MnW_{11}\}$	0.27 ± 0.01	1.19 ± 0.21	84.42

<sup>a</sup> Conditions: [catalyst] = 4.0  $\mu$ M, [BB41]<sub>0</sub> = 20  $\mu$ M, monochromatic 390 nm LED irradiation; <sup>b</sup> Percent decrease of the deaerated, irradiated sample compared with the aerated, irradiated sample (Table 2).

Further photocatalytic reactions were performed in the presence of the hydroxyl radical scavenger (EtOH) to establish whether hydroxyl radicals are involved in the photooxidation mechanism. To this end, the standard photooxidation reaction was performed in the presence of ethanol ([EtOH]: [BB41]: [cluster] = 50:5:1). The experiments were performed under aerated conditions. For all  $\{MW_{11}\}$  catalysts, a significant decrease in photo oxidative activity between ca. 81 and ca. 98 % is observed, see Table 4 and Figure 5, suggesting that hydroxyl radical formation is indeed the basis of the photooxidation mechanism for the catalysts under investigation. Further, it was demonstrated that EtOH acts only as quencher and not as reductant, as no reaction between the photoexcited POMs and EtOH was observed, see SI. Based on earlier studies, we hypothesized that traces of water in the solvent are the source of hydroxyl radicals. This was supported by reference experiments using dry DMF which showed that the reaction rate dropped drastically (see ESI).

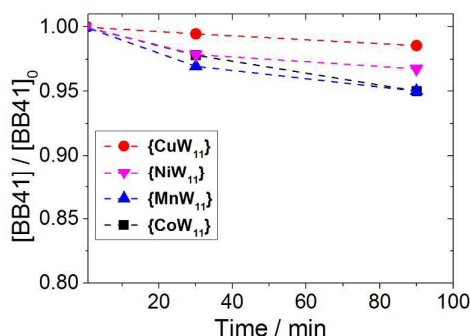


**Figure 5** { $MW_{11}$ }-catalyzed photooxidation of BB41 in the presence of the hydroxyl radical scavenger ethanol. Conditions: aerated DMF solution; [EtOH]: [BB41]: {[ $MW_{11}$ ]} = 50:5:1, 390 nm LED irradiation.

**Table 4:** Observed rate constants of BB41 photodegradation by { $MW_{11}$ } in the presence of the hydroxyl radical scavenger ethanol.<sup>a</sup>

No	Cluster	Irradiated, no scavenger $k_{obs}$ / $10^{-8}$ M min <sup>-1</sup>	Irradiated, scavenger present $K_{obs}$ / $10^{-8}$ M min <sup>-1</sup>	Percent decrease <sup>b</sup>
1	{CuW <sub>11</sub> }	4.66 ± 0.13	0.10 ± 0.02	97.85
2	{CoW <sub>11</sub> }	5.17 ± 0.17	0.40 ± 0.06	92.26
3	{NiW <sub>11</sub> }	5.33 ± 0.28	0.85 ± 0.07	84.05
4	{MnW <sub>11</sub> }	9.59 ± 0.34	1.78 ± 0.12	81.44

<sup>a</sup> Conditions: [catalyst] = 4.0 μM, [BB41]<sub>0</sub> = 20 μM, monochromatic 390 nm LED irradiation, scavenger: EtOH, [EtOH] = 200 μM; <sup>b</sup> Percent decrease of the scavenger-containing solution compared to the scavenger-free solution.

## Conclusions

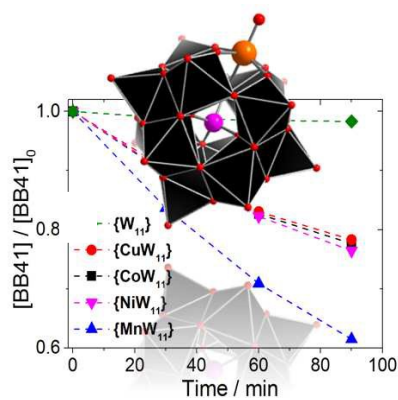
In conclusion, we report that mono-metal-functionalized lacunary tungstate clusters show photoactivity in the near-UV-Vis region for photooxidative dye degradation. Distinct reactivity differences are observed depending on the type of metal employed, highlighting that metal functionalization is a suitable tool for tuning the cluster photoreactivity. Initial mechanistic studies show that oxygen is required as a re-oxidant for efficient photocatalysis and that the catalytic cycle proceeds via the intermediate formation of hydroxyl radicals which act as oxidant to degrade the dye. Future studies will investigate the underlying photophysical properties in more detail to understand the effects of different metals on the initial steps of the photoexcitation.

## Acknowledgements

Financial support by Schlumberger foundation Faculty for the future program, by the Graduate school GRK1626 "Chemical Photosynthesis" (Regensburg University) and by the Institute of Inorganic Chemistry I (Ulm University) is gratefully acknowledged.

## Notes and references

- special POM-themed issue: L. Cronin and A. Müller (guest eds.), *Chem. Soc. Rev.*, 2012, **41**, 7325–7648.
- Special POM issue: C. L. Hill (guest ed.), *Chem. Rev.*, 1998, **98**, 1–390.
- M. T. Pope and A. Müller, *Angew. Chem. Int. Ed. Engl.*, 1991, **30**, 34–48.
- C. L. Hill and C. M. Prosser-McCarthy, *Coord. Chem. Rev.*, 1995, **143**, 407–455.
- C. Streb, *Dalton Trans.*, 2012, **41**, 1651–1659.
- A. Müller, P. Kögerler and A. W. M. Dress, *Coord. Chem. Rev.*, 2001, **222**, 193–218.
- D. L. Long, R. Tsunashima and L. Cronin, *Angew. Chem. Int. Ed.*, 2010, **49**, 1736–1758.
- H. Lv, Y. V. Geletii, C. Zhao, J. W. Vickers, G. Zhu, Z. Luo, J. Song, T. Lian, D. G. Musaev and C. L. Hill, *Chem. Soc. Rev.*, 2012, **41**, 7572–7589.
- T. Yamase, *Catal. Surv. Asia*, 2003, **7**, 203–217.
- J. Forster, B. Rösner, M. M. Khusniyarov and C. Streb, *Chem. Commun.*, 2011, **47**, 3114–3116.
- B. Matt, X. Xiang, A. L. Kaledin, N. Han, J. Moussa, H. Amouri, S. Alves, C. L. Hill, T. Lian, D. G. Musaev, G. Izzet and A. Proust, *Chem. Sci.*, 2013, **4**, 1737.
- J. Tucher, L. C. Nye, I. Ivanovic-Burmazovic, A. Notarnicola and C. Streb, *Chem. Eur. J.*, 2012, **18**, 10949–10953.
- B. S. Jaynes and C. L. Hill, *J. Am. Chem. Soc.*, 1993, 12212–12213.
- J. Tucher, S. Schlicht, C. Streb, F. Kollhoff and C. Streb, *Dalton Trans.*, 2014, **43**, 17029–17033.
- J. Tucher, Y. Wu, L. C. Nye, I. Ivanovic-Burmazovic, M. M. Khusniyarov and C. Streb, *Dalton Trans.*, 2012, **41**, 9938.
- M. T. Pope, *Heteropoly and isopoly oxometalates*, Springer, Berlin, 1983.
- T. J. R. Weakley and S. A. Malik, 1967, **29**, 2935–2944.
- S. H. Szczepankiewicz, C. M. Ippolito, B. P. Santora, T. J. van de Ven, G. A. Ippolito, L. Fronckowiak, F. Wiatrowski, T. Power and M. Kozik, *Inorg. Chem.*, 1998, **37**, 4344–4352.
- C. M. Tourné, G. F. Tourné, S. A. Malik and T. J. R. Weakley, *J. Inorg. Nucl. Chem.*, 1970, **32**, 3875–3890.
- R. Neumann and C. Abu-Gnim, *J. Am. Chem. Soc.*, 1990, **112**, 6025–6031.
- S. Herrmann, M. Kostrzewa, A. Wierschem and C. Streb, *Angew. Chem. Int. Ed.*, 2014, **53**, 13596–13599.
- M. K. Saini, R. Gupta, S. Parbhakar, A. Kumar Mishra, R. Mathur and F. Hussain, *RSC Adv.*, 2014, **4**, 25357–25364.
- J. Tucher, K. Peuntinger, J. T. Margraf, T. Clark, D. M. Guldi and C. Streb, *Chem. Eur. J.*, 2015, **21**, 8716–8719.
- J. Tucher and C. Streb, *Beilstein J. Nanotechnol.*, 2014, **5**, 711–716.
- A. Seliverstov and C. Streb, *Chem. Eur. J.*, 2014, **20**, 9733–9738.



The photooxidative activity of mono-transition-metal functionalized lacunary silicotungstate Keggin anions is reported together with preliminary mechanistic insight into the photoreactivity.